

## **Supporting Information**

### **Solid-State-Ligand-Exchange Free Quantum Dot Ink-based Solar Cells with Efficiency of 10.9%**

Havid Aqoma, Sung-Yeon Jang\*

*Department of Chemistry, Kookmin University, 77 Jeongneung-ro, Seongbuk-gu, Seoul 136-702, Republic of Korea. E-mail: syjang@kookmin.ac.kr*

## Experimental

### CQDs synthesis

The iodide-treated oleate-capped CQDs were synthesized using previously published methods with a slight modification.<sup>1</sup> Lead oxide (1.88 g, 99.99%, Sigma-Aldrich) and oleic acid (7 mL, technical grade 90%, Sigma-Aldrich) were dissolved in 1-octadecene (40 mL, technical grade 90%, Sigma-Aldrich) under vacuum conditions in a three-necked flask, at 110 °C for 2 h. The bis(trimethylsilyl)sulfide (720  $\mu$ L, synthetic grade, Sigma-Aldrich) was mixed with 1-octadecene (10 mL) to prepare the sulfur precursor. The sulfur precursor was quickly injected into the reaction flask under N<sub>2</sub> at 115 °C, held for around 2 s, and the flask was then moved to the water bath and injected with toluene (30 mL) for thermal quenching. The precipitation of the CQDs was obtained by the addition of 100 mL of acetone, and then were centrifuged. The solid CQDs were dissolved in 45 mL of toluene and moved to a three-necked flask under N<sub>2</sub> condition for iodide treatment. The iodide precursor was prepared by dissolving tetrabutylammonium iodide (1.1 g, Sigma-Aldrich) in oleylamine (10 mL) at 200 °C for 2 h under N<sub>2</sub> in a Schlenk line, and then under vacuum at 100 °C for 2 h, finally kept at 40 °C. 2 mL of the iodide precursor was injected into the untreated CQDs dropwise, and stirred at room temperature for 15 min. Methanol (135 mL) was added to the precipitated CQDs, and the solution was centrifuged. Dissolving and precipitation by toluene and methanol was repeated one more time. After drying the residual solvent for 3 hours in vacuum, CQDs was dissolved in octane. The un-treated oleate-capped CQDs were prepared by skipping the iodide treatment process.<sup>2</sup>

### Synthesis of nQD-ink by PTE

The procedure follows the reported method with a slight modification.<sup>3,4</sup> The 5 mL of DMF, which contained 0.5 mmol PbI<sub>2</sub>, 0.1 mmol PbBr<sub>2</sub>, and 0.2 mmol ammonium acetate, was mixed vigorously with 5 mL of the iodide-treated oleate-capped CQDs octane solution (10 mg/mL) at 35 °C. After 15 mins, the CQDs were completely transferred to the DMF phase. The CQDs in the DMF solution were washed with octane two times and precipitated by the addition of ~2.7 mL of toluene. After the solid CQDs were separated by centrifugation, the CQDs were dried in vacuum oven for 15 mins. Butylamine was added to the CQDs to yield 150 mg/mL of the nQD-ink.

### Synthesis of pQD-ink by PTE

3 mL of o-CQDs solution in octane (8 mg/mL), synthesized by a reported method,<sup>5</sup> was mixed with 12.6 mM of MPA in 3 mL of dimethylformamide (DMF) followed by brief shaking (~10 s). The CQDs were transferred from the octane to the DMF, and immediately centrifuged to collect the solid CQDs. After drying in ambient condition for 10 min, the solid CQDs were dispersed in aqueous solvents (Figure 1). For the default aqueous solvent (water:BA, 95:5) of pQD-ink, 114  $\mu$ L of water and 6  $\mu$ L of BA were used for 24 mg of CQDs. The pQD-ink showed sufficient dispensability at concentrations up to 200 mg/mL.

### Ink-device fabrication

The ITO/glass substrates were cleaned by sonication in acetone and isopropyl alcohol for 20 min each, and then dried at 120 °C in vacuum oven overnight. The ZnO buffer layer was prepared following our previously reported method.<sup>3</sup> The nQD-ink solution (150 mg/mL) was spin coated on the ZnO layers at 800 rpm for 40 s, followed by drying at 105 °C for 1 min. On the nQD-ink layer, the pQD-ink (80 mg/mL in water with 5% of BA) was spin coated at 2500 rpm for 40 s, and dried at 105 °C for 1 min. For the pQD-SSE layer preparation, o-CQDs in octane (40 mg/mL) were spin coated at 2000 rpm for 10 s, followed by ligand exchange with 0.04% v/v of MPA in acetonitrile for 30 s. After washing with neat

acetonitrile 2 times, the pQD-SSE layer was dried at 95 °C for 1 min. Finally, an Au electrode with a thickness of 80 nm was thermally deposited at reduced pressure ( $10^{-6}$  torr). The inverted CQD devices, using pQD-ink as the active layer, were fabricated following the reported procedure.<sup>2</sup> The PEDOT:PSS (Clevios AI4083, H. C. Starck) was diluted in MeOH (1/1 v/v), then spin coated on the ITO with 4000 rpm for 35 s. Thermal annealing of PEDOT:PSS films was performed at 120 °C for 15 min. The active layer was prepared by spin coating pQD-ink (200 mg/mL) at 800 rpm for 80 s, followed by drying at 95 °C for 1 min.

### Doctor-blade coating of CQD films

The blade coating process was performed in air atmosphere using a home-made blade coater, and the blading process was performed manually with the speed of approximately 2.5–3 cm/s. The nQD-ink (150 mg/mL) in a mixed solvent (DMF/BA, 1/1 volume ratio) was blade-coated on ZnO layers or glass substrates with a 0.3 mm gap between blade and substrate, followed by drying at 105 °C for 1 min in ambient air. The thickness of the bladed nQD-ink layers was ~450 nm. The aqueous pQD-ink (40 mg/mL) in water with 5% of BA was blade-coated on the nQD-ink layer or glass substrates with 0.2 mm gap between blade and substrate, followed by drying at 105 °C for 1 min in ambient air. The temperature and humidity for the blade coating process were 20–23 °C and 30% respectively. The bladed devices with active areas of 0.126 cm<sup>2</sup> were fabricated using a corresponding evaporator mask. The PCEs of the devices with active areas of 0.252 cm<sup>2</sup> and 0.504 cm<sup>2</sup> were determined by electrically connecting two and four of the devices with active area of 0.126 cm<sup>2</sup> in the same substrate.

### Characterizations:

Field-emission scanning electron microscopy (FE-SEM, JEOL JSM-7610F) was used to measure cross-sectional images of the devices. Electrophoretic light scattering (ELS-Z2, Otsuka Ltd) was used to analyze the zeta potential of the CQDs solution. The concentration of the measured CQD solution and inks was maintained at 0.2 mg/mL. UPS was carried out using an AXIS-NOVA (Kratos) system with HeI and a base pressure of  $5 \times 10^{-8}$  Torr. The samples were coated on Au substrates. X-ray photoelectron spectroscopy (XPS) was performed using a MultiLab 2000 (THERMO VG SCIENCE) system with a base pressure of  $1 \times 10^{-9}$  Pa and monochromatized MgK $\alpha$  with 1253.6 eV. The binding energies were calibrated using the C 1s peak at 285.0 eV. The samples were coated on Ag substrates. Photoluminescence (PL) measurements were carried out using a Horiba FL3-2iHR spectrometer with InGaAs detector arrays. The excitation for PL measurement was 400 nm. The  $J$ - $V$  characteristics of the solar cells were recorded using a Keithley 2401 source unit under AM 1.5G one sun illumination in ambient air condition. The light intensity was calibrated using monosilicon standard cells calibrated by the National Renewable Energy Laboratory (NREL). The  $J$ - $V$  curves were obtained through backward scan (0.8 V  $\rightarrow$  -0.1 V) with 40 mV step size and 0.1 s delay time; forward scan (-0.1 V  $\rightarrow$  0.8 V) was performed in the same condition. A black shadow mask with an area of 5.18 mm<sup>2</sup> was used to define the active area.<sup>6</sup> The  $J$ - $V$  measurements of the devices were performed in ambient air environment after one day of fabrication. The EQE spectra was measured using monochromated light with a 5 Hz chopper frequency (McScience, K3100 IQX), and a silicon photodiode was used as a reference. The morphology of CQD surface was measured by atomic force microscope (AFM) using tapping mode on Nanoscope instrument (Bruker). Intensity modulated photovoltage spectroscopy (IMVS) were performed using an impedance analyzer (IVIUM Tech., IviumStat). The DC and AC components of the illumination source were provided by a blue emission LED ( $\lambda = 460$  nm) with 50% modulation depth of the AC component superimposed on the DC light. Open-circuit conditions were used for IMVS measurement. The mean recombination time ( $\tau_r$ ) of photogenerated charges were acquired from the minimum frequency in the Nyquist plot of IMVS results by  $\tau_r = (2\pi f_{\min})^{-1}$ .

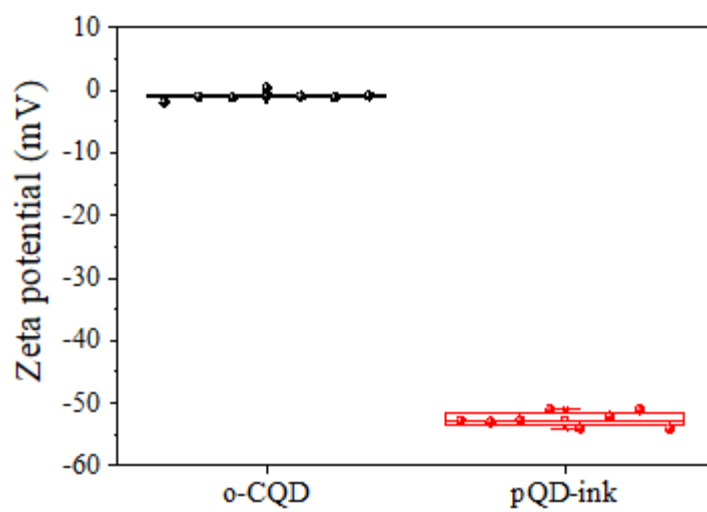


**Figure S1.** Statistics of the  $\zeta$ -potential values of the o-CQD solution and pQD-inks.

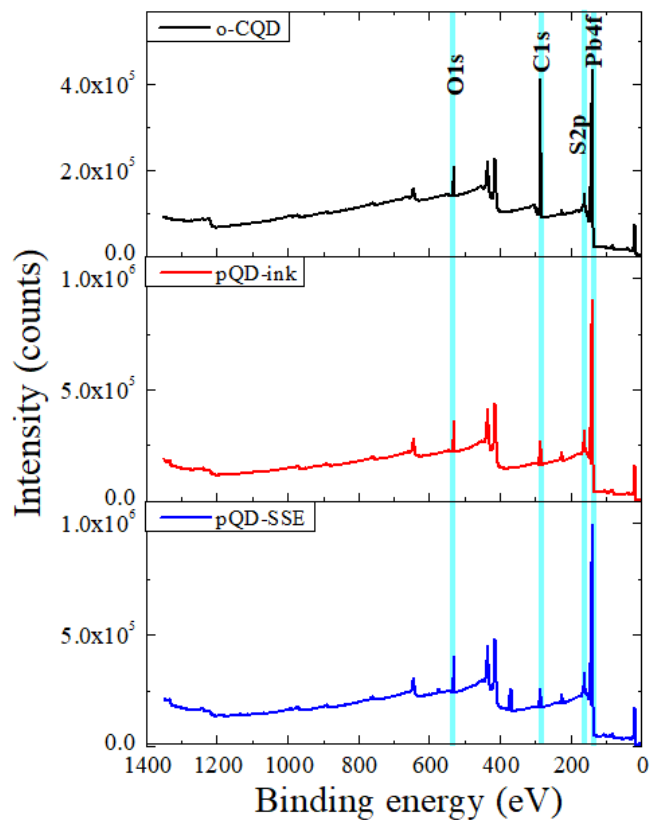


**Figure S2.** Wide-scan XPS spectra of various CQDs.

**Table S1.** Atomic ratio of various CQDs from XPS spectra analysis.

	<b>Pb 4f</b>	<b>S 2p</b>	<b>O 1s</b>	<b>C 1s</b>
o-CQD	1.00	0.63	0.74	8.85
pQD-ink	1.00	1.00	0.54	1.57
pQD-SSE	1.00	0.97	0.58	1.46

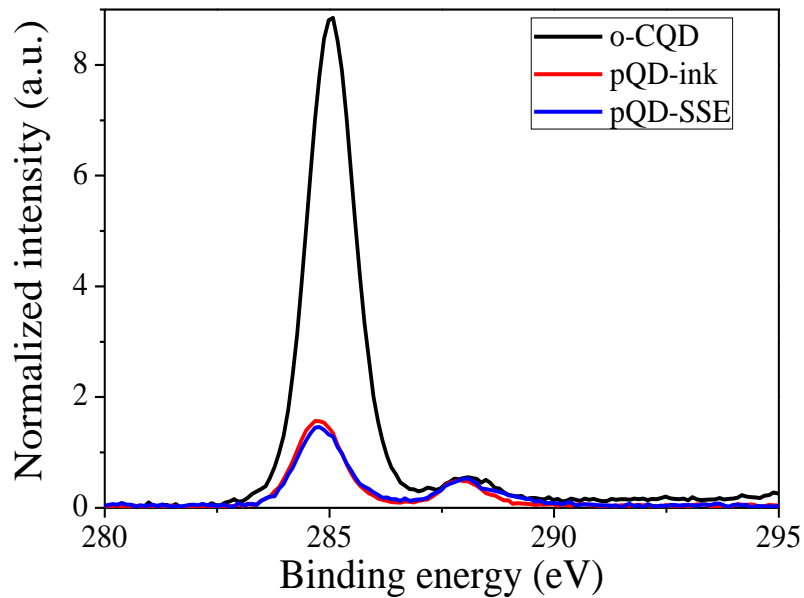


**Figure S3.** Normalized C 1s XPS spectra of various CQD films.

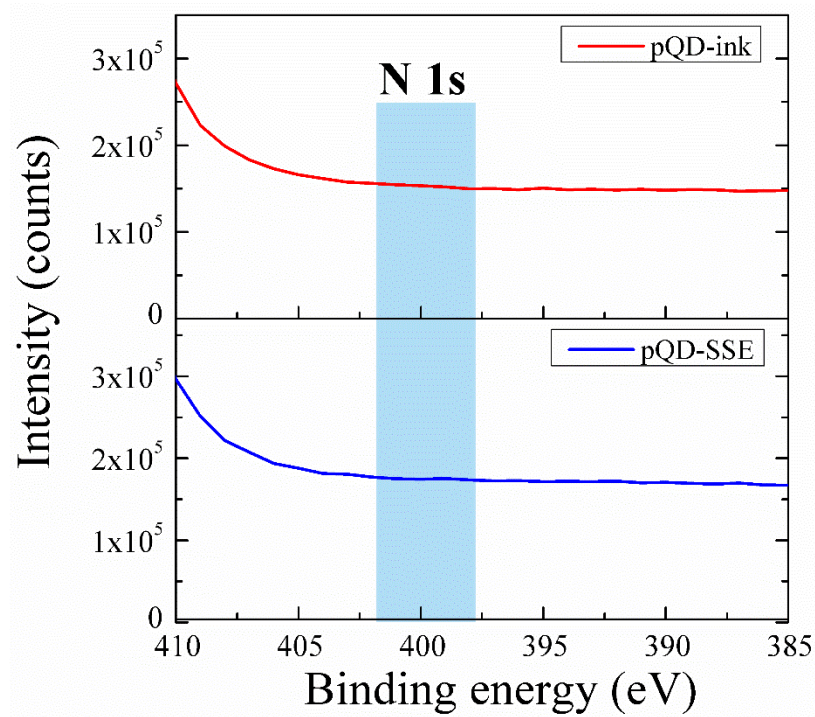
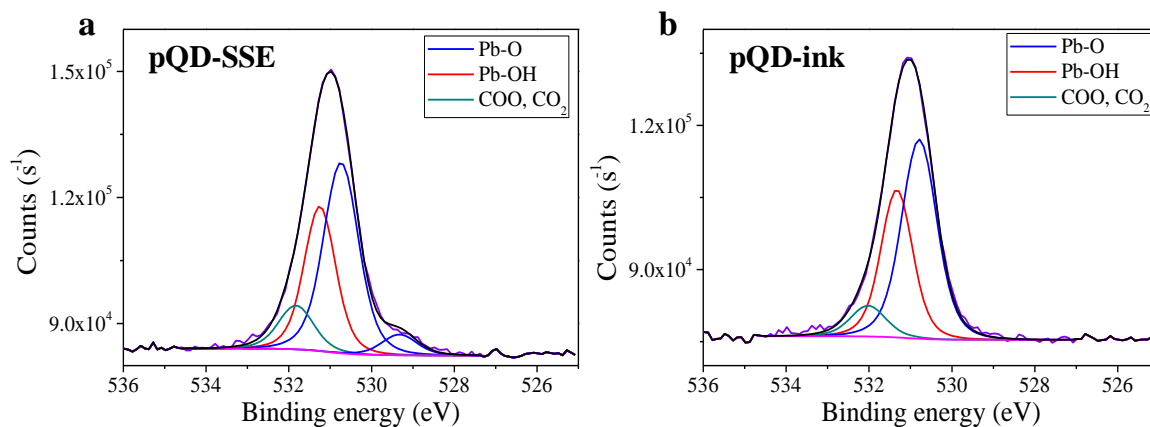


**Figure S4.** N 1s XPS spectra of the pQD films.



**Table S2.** Component ratio from deconvoluted S 2*p* peaks in Figure 2d

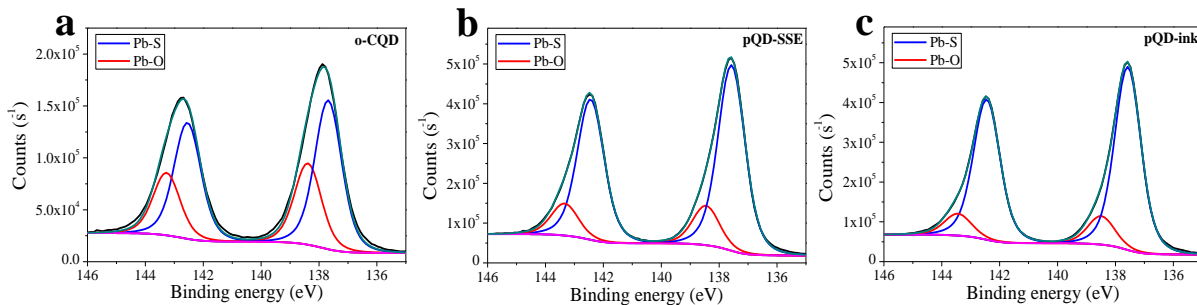
<b>PbS-CQD</b>	<b>Component</b>	<b>Peak (eV)</b>	<b>FWHM</b>	<b>Area (%)</b>	<b>Component ratio</b>
<b>pQD-SSE</b>	Pb-S	160.6	1.0	57.71	0.56
		161.9	0.9		
	bound thiolate	161.6	1.0	28.71	0.28
		162.5	1.0		
		unbound thiolate	163.3	1.0	13.58
		164.6	1.1		
<b>pQD-ink</b>	Pb-S	160.6	1.0	56.00	0.56
		162.0	0.9		
	bound thiolate	161.6	0.9	27.96	0.28
		162.9	0.9		
		unbound thiolate	163.4	0.9	16.04
		164.6	1.2		



**Figure S5.** XPS analysis result of O 1s of **a**, pQD-SSE and **b**, pQD-ink CQD film.

**Table S3.** Component ratio from deconvoluted O 1s peaks in Figure S5.

PbS-CQD	Component	Peak (eV)	FWHM	Area (%)	Component ratio
pQD-SSE	Pb-O	529.3	1	5.37	0.03
	Pb-O	530.7	1	49.46	0.29
	Pb-OH	531.2	0.9	33.79	0.20
	COO	531.8	1	11.39	0.07
pQD-ink	Pb-O	530.8	1	54.88	0.29
	Pb-OH	531.3	0.9	36.64	0.20
	COO	532.0	1	8.48	0.05

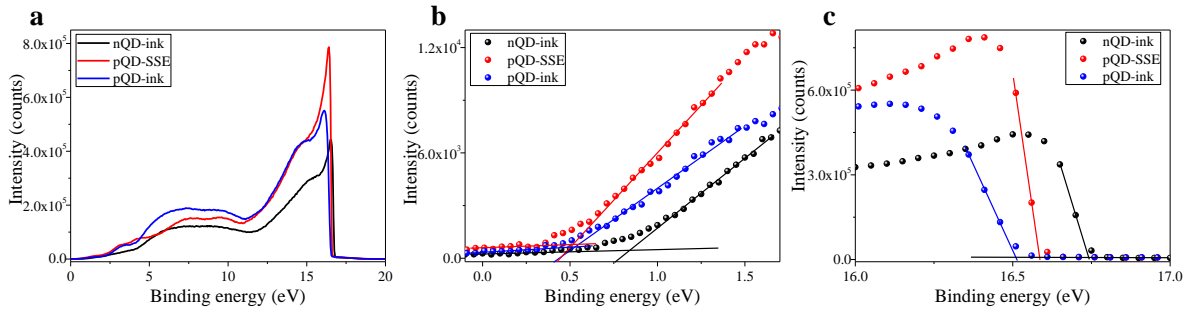


**Figure S6.** XPS analysis results of Pb 4f of **a**, o-CQD, **b**, pQD-SSE, **c**, pQD-ink.



**Table S4.** Deconvoluted component from Pb 4*f* peaks in Figure S6.

PbS-CQD	Component	Peak (eV)	FWHM	Area (%)
o-CQD	Pb-S	137.7	1.1	36.31
	Pb-S	142.5	1.1	28.39
	Pb-O	138.4	1.1	33.79
	Pb-O	143.2	1.1	11.39
pQD-SSE	Pb-S	137.6	1.1	46.72
	Pb-S	142.4	1.1	35.33
	Pb-O	138.4	1.1	9.88
	Pb-O	143.3	1.1	8.06
pQD-ink	Pb-S	137.6	1.1	48.54
	Pb-S	142.4	1.1	37.70
	Pb-O	138.5	1.1	7.79
	Pb-O	143.4	1.1	5.97

**Figure S7.** UPS spectra analysis for various CQD films.

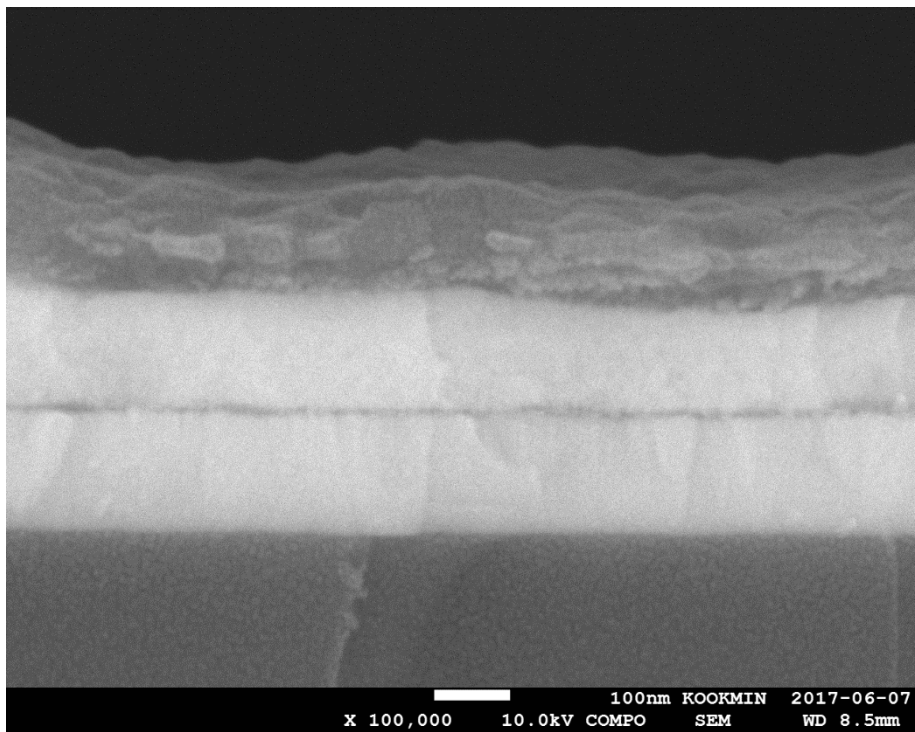


**Figure S8.** Cross-sectional FE-SEM image of the device in Figure 2f.

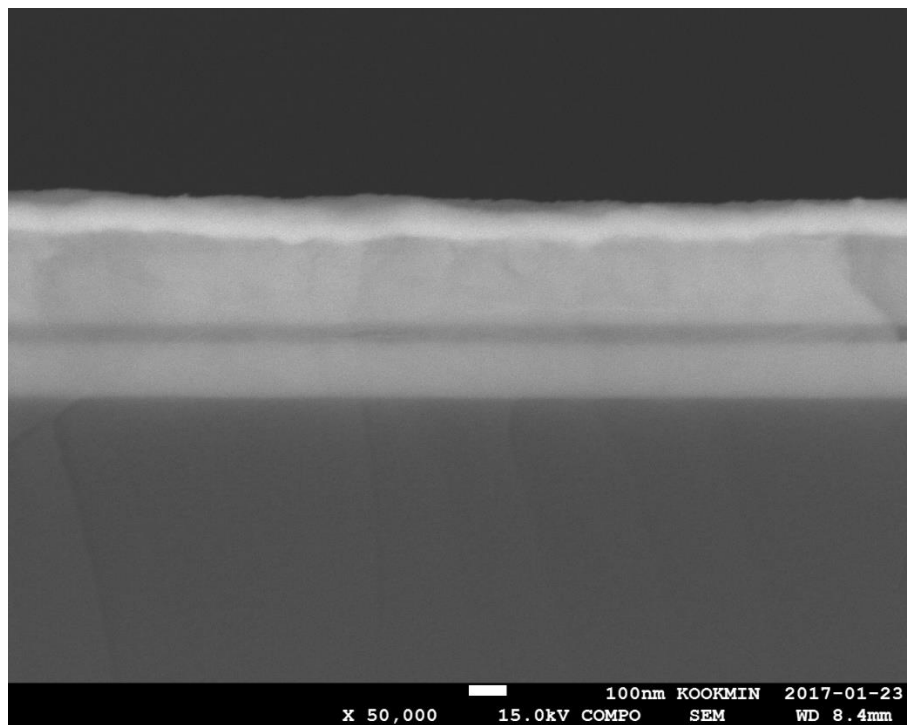


**Figure S9.** Cross-sectional FE-SEM image of the device in Figure 3a.

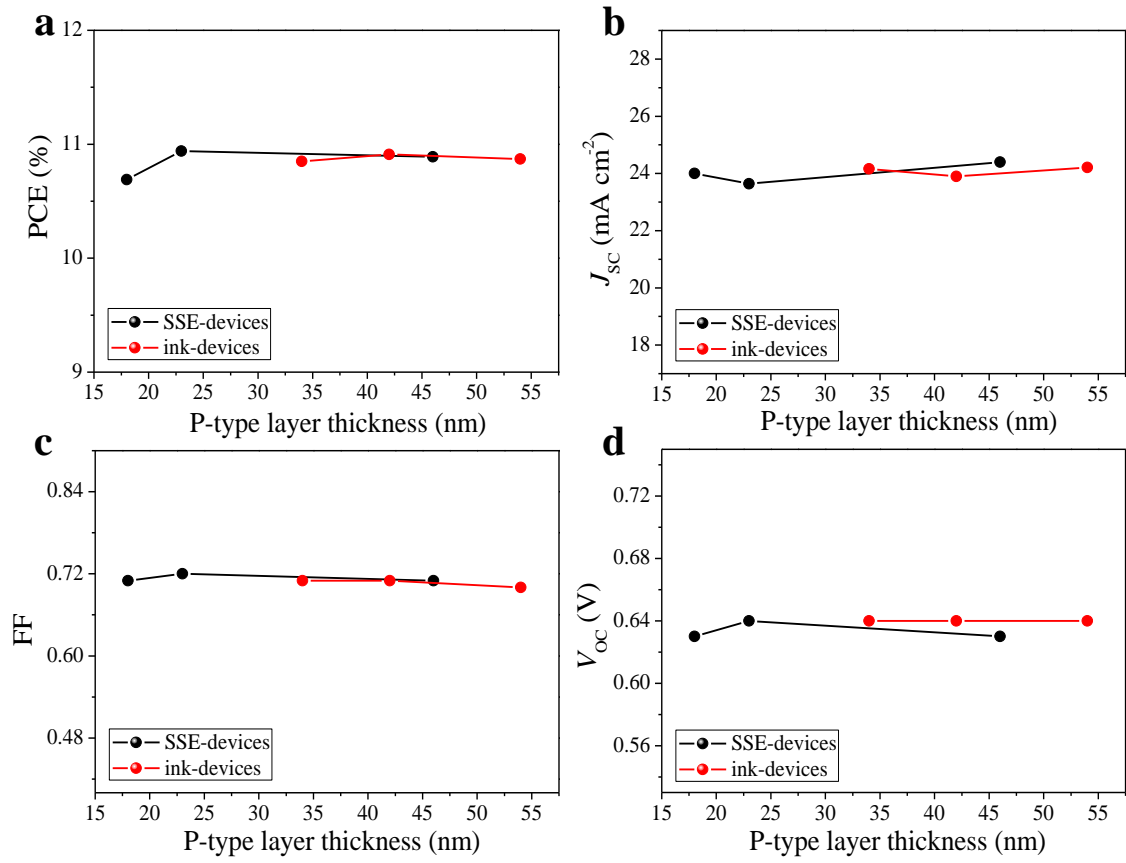


**Figure S10.** Device performance with various p-type CQD layer thicknesses. The thickness of the nQD-ink layers was fixed at ~220 nm.

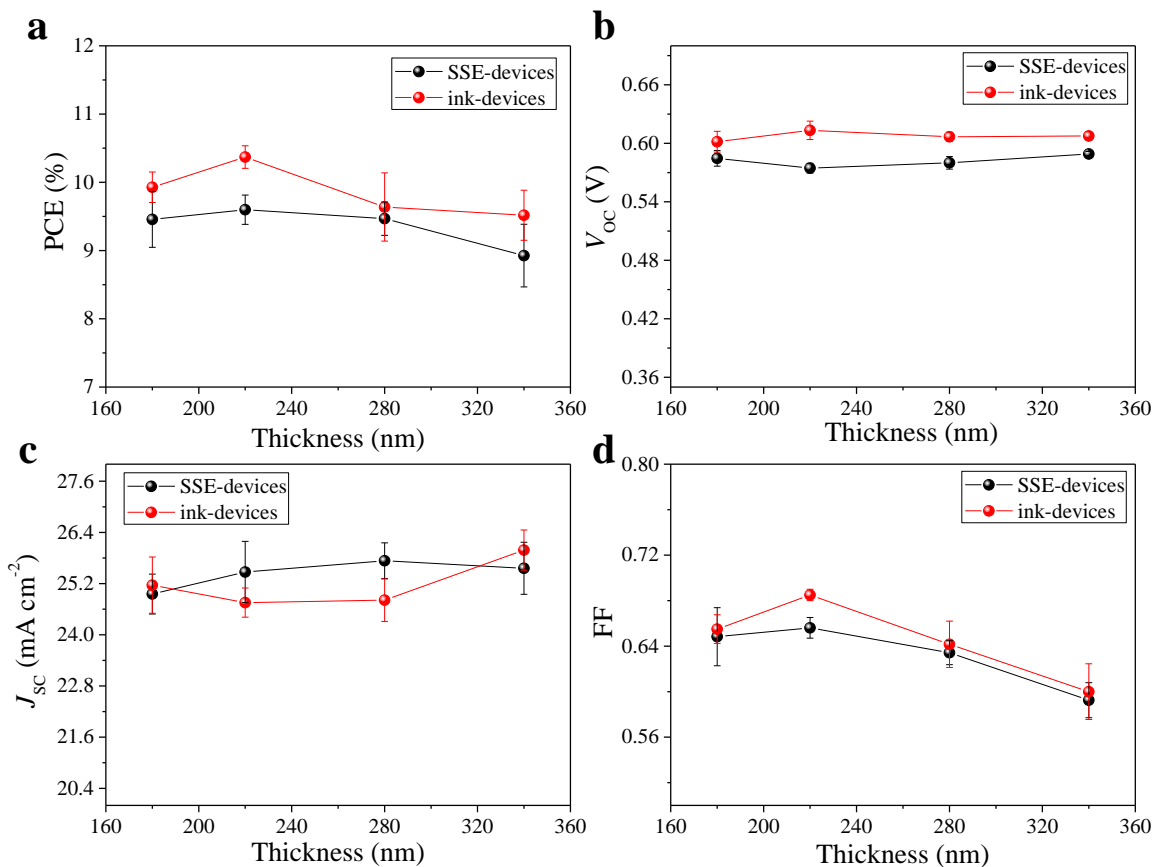


**Figure S11.** Device performance with various nQD-ink active layer thicknesses. The thickness of the pQD-ink layers was fixed at ~40 nm.

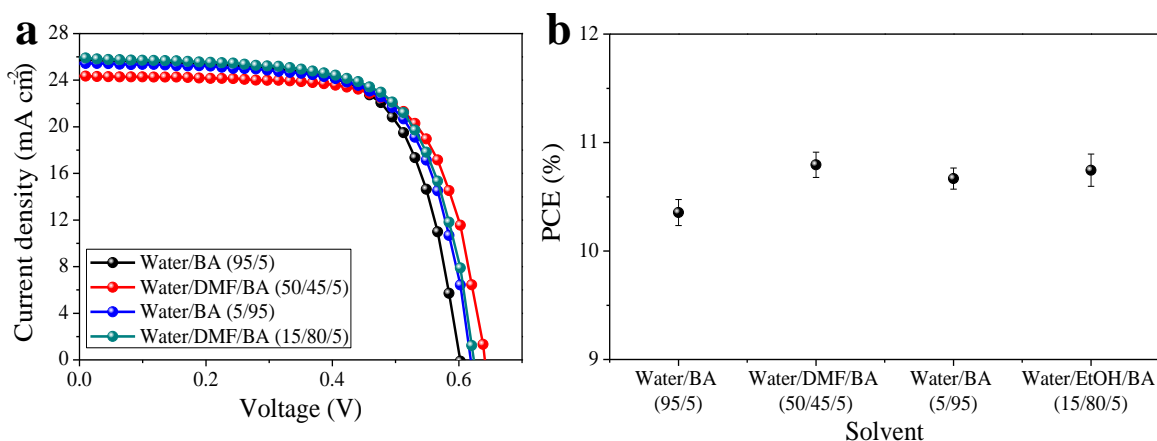


**Figure S12.** The performance of devices using pQD-ink solution in various solvent systems. (6 devices for each condition).

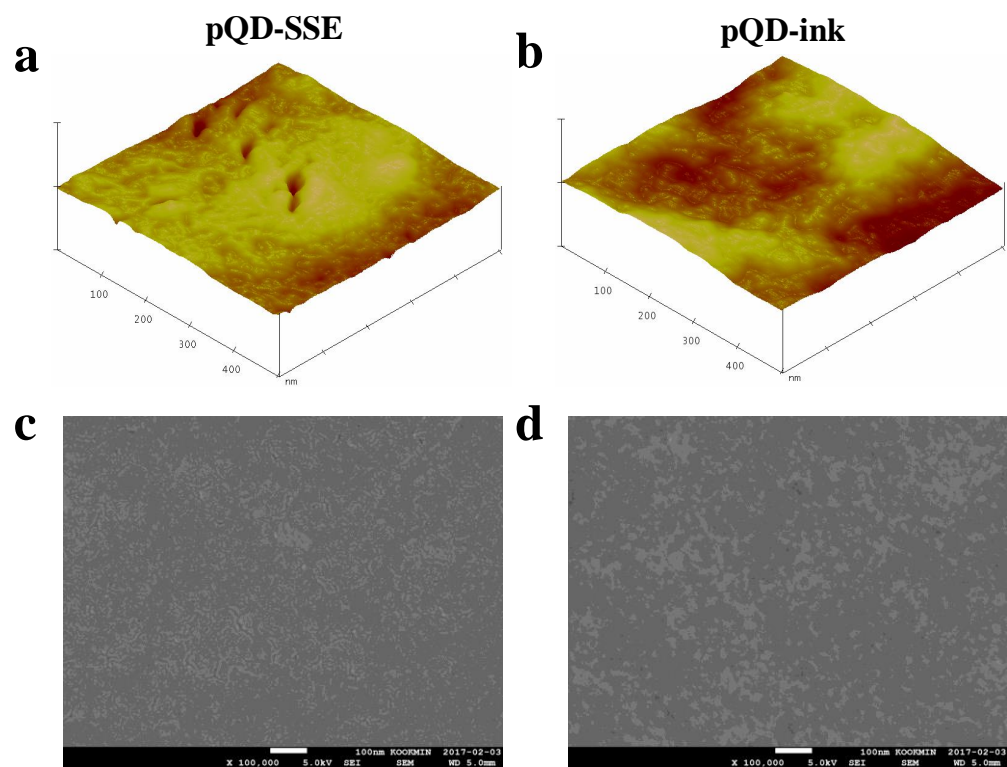


**Figure S13.** AFM images (a-b) and SEM images (c-d) of pQD-SSE film and pQD-ink film.

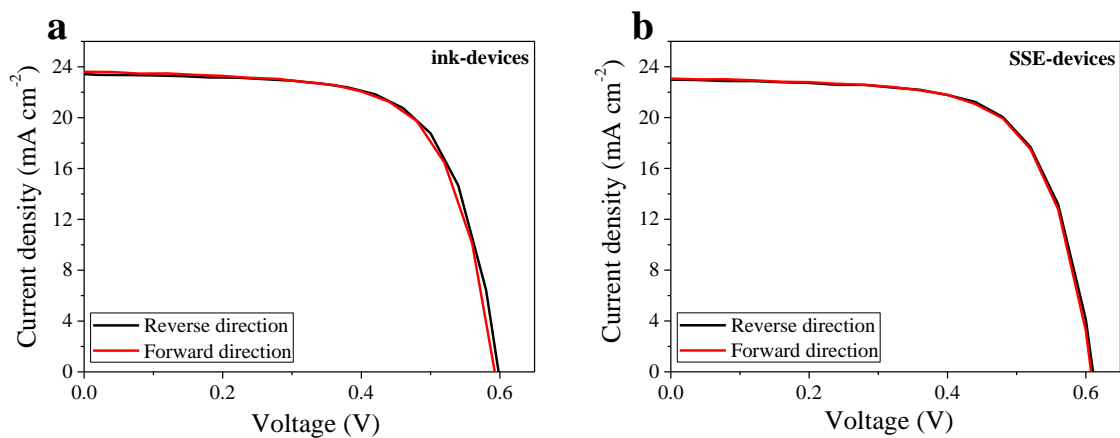


**Figure S14.** Hysteresis in the  $J$ - $V$  characteristics of the devices.

**Table S5.** Summary of device performance in Figure S14.

Device	Scan direction	PCE (%)	$V_{oc}$ (V)	$J_{sc}$ ( $\text{mA cm}^{-2}$ )	FF
SSE-devices	Reverse	9.61	0.61	22.99	0.69
	Forward	9.57	0.61	23.07	0.68
ink-devices	Reverse	9.55	0.60	23.43	0.68
	Forward	9.47	0.59	23.61	0.68

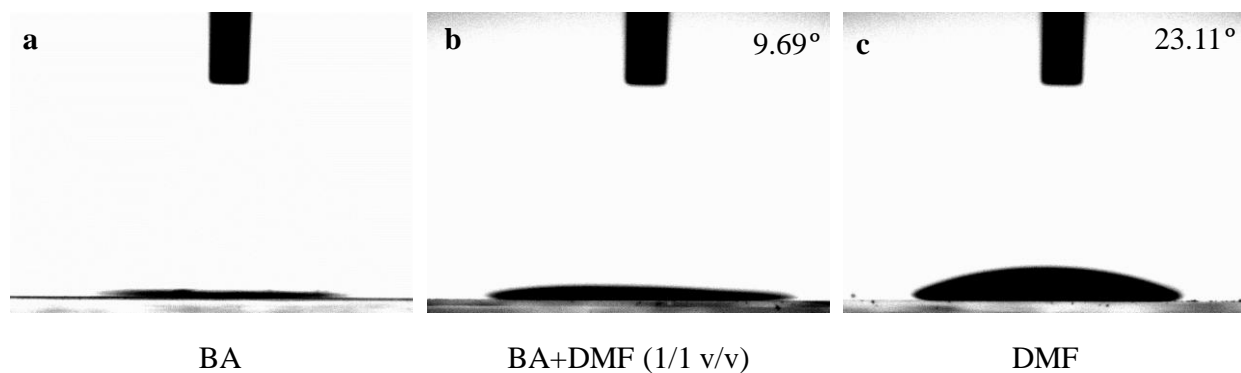


**Figure S15.** Contact angle measurement of nQD-ink on top of ZnO with various solvent compositions.

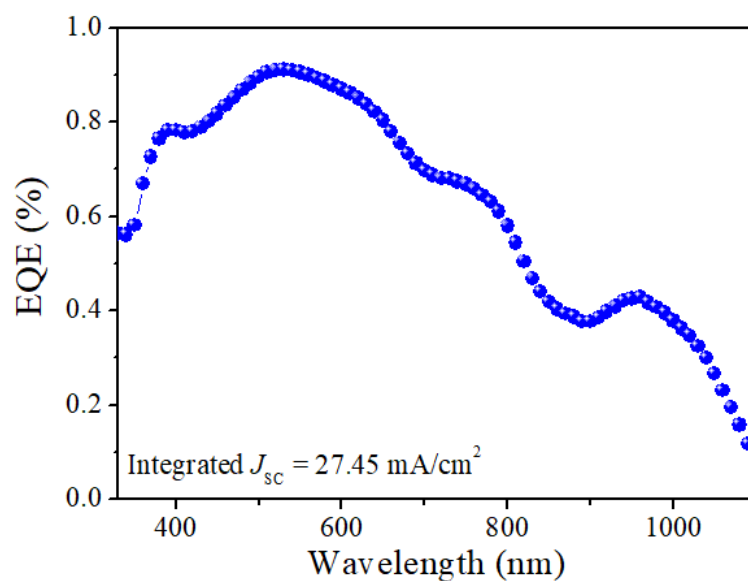


**Figure S16.** IPCE spectra of the champion blade coated device

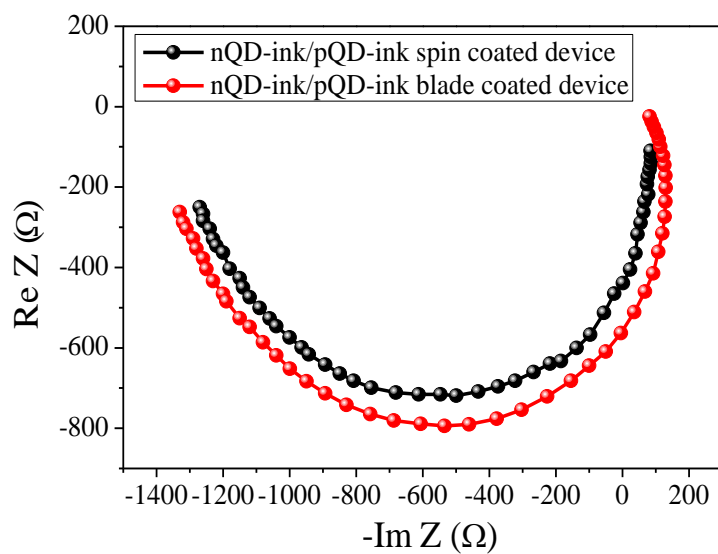


**Figure S17.** Intensity modulated photovoltage spectroscopy (IMVS) analysis results of bladed device and spin-coated device.

**Table S6.** Summary device characterization results in Figure S17.

	IMVS	
	$f_{\min}$	$\tau_{\text{lifetime}}$ (ns)
nQD-ink/pQD-ink spin coated device	$3.13 \times 10^4$	$5.09 \times 10^3$
nQD-ink/pQD-ink blade coated device	$3.24 \times 10^4$	$4.91 \times 10^3$

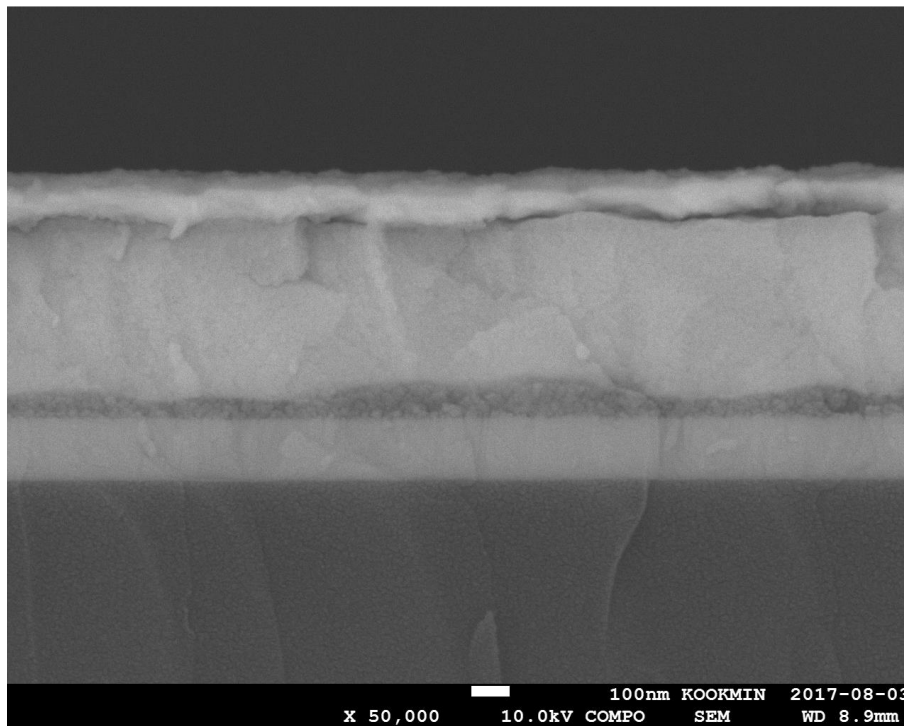


**Figure S18.** Cross-sectional FE-SEM image of the blade coated device.

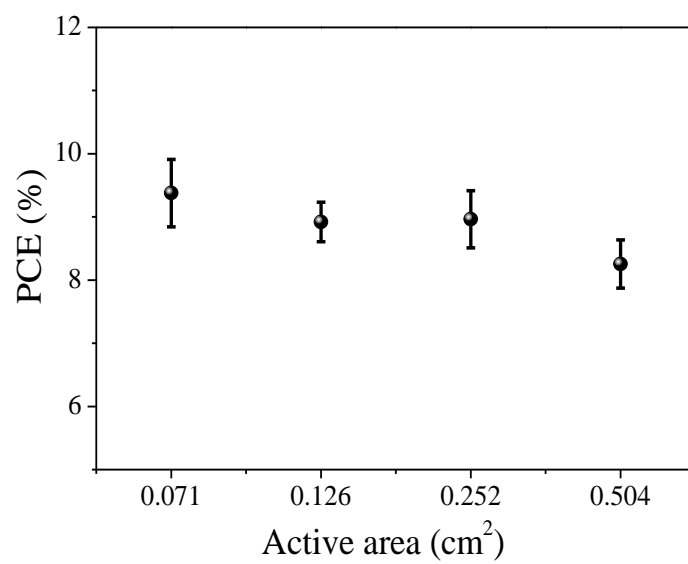


**Figure S19.** The performance of blade-coated devices with higher active areas.

## References

- 1 Z. Ning, O. Voznyy, J. Pan, S. Hoogland, V. Adinolfi, J. Xu, M. Li, A. R. Kirmani, J. P. Sun, J. Minor, K. W. Kemp, H. Dong, L. Rollny, A. Labelle, G. Carey, B. Sutherland, I. Hill, A. Amassian, H. Liu, J. Tang, O. M. Bakr and E. H. Sargent, *Nat. Mater.*, 2014, **13**, 822-828.
- 2 H. Aqoma, N. Barange, I. Ryu, S. Yim, Y. R. Do, S. Cho, D. H. Ko and S. Y. Jang, *Adv. Funct. Mater.*, 2015, **25**, 6241-6249.
- 3 H. Aqoma, M. Al Mubarak, W. T. Hadmojo, E. H. Lee, T. W. Kim, T. K. Ahn, S. H. Oh and S. Y. Jang, *Adv. Mater.*, 2017, **29**, 1605756.
- 4 M. Liu, O. Voznyy, R. Sabatini, P. F. de Arquer, R. Munir, A. Balawi, X. Lan, F. Fan, G. Walters, A. R. Kirmani, S. Hoogland, F. Laquai, A. Amassian and E. H. Sargent, *Nat. Mater.*, 2016, **16**, 258-263.
- 5 M. A. Hines and G. D. Scholes, *Adv. Mater.*, 2003, **15**, 1844-1849.
- 6 R. Azmi, S. H. Oh and S. Y. Jang, *ACS Energy Lett*, 2016, **1**, 100-106.